Catalysis
Science & Technology

Cite this: *Catal. Sci. Technol.*, 2011, **1**, 1006–1012

www.rsc.org/catalysis

PAPER

Catalytic performance of $La_{1-x}Er_xCoO_3$ perovskite for the deoxidization of coal bed methane and role of erbium in a catalyst

Zhicong Liu,[a] Guanzhong Lu,*[ab] Yun Guo,[a] Yanqin Wang[a] and Yanglong Guo[a]

Received 20th April 2011, Accepted 11th May 2011
DOI: 10.1039/c1cy00140j

The effective utilization of coal bed methane (CBM) is very significant for energy utilization and environmental protection, reducing significantly greenhouse gas methane emission. In this paper, $La_{1-x}Er_xCoO_3$ perovskite ($0 \leq x \leq 0.4$) catalysts for the catalytic deoxidization of CBM were prepared by a co-precipitation method and were characterized by X-ray diffraction (XRD), laser Raman spectroscopy (LRS), H_2 and CH_4 temperature-programmed reduction (H_2, CH_4-TPR), CO pulse and N_2 adsorption/desorption techniques. The results show that the amount of Er affects obviously the physicochemical and catalytic properties of $La_{1-x}Er_xCoO_3$, and when $x = 0.2$, $La_{0.8}Er_{0.2}CoO_3$ exhibits the best activity for deoxidization of CBM, because Er doping promotes the activity and migration of the lattice oxygen of $La_{0.8}Er_{0.2}CoO_3$. The influences of the operation parameters (methane concentration, oxygen concentration and space velocity) on the catalytic deoxygenation of CBM and the kinetics behaviours were investigated. The reaction order of removing oxygen is 0.9 for methane partial pressure and −0.6 for oxygen partial pressure.

1. Introduction

Coal bed methane (CBM), also known as coal mine gas and coal seam gas, is a kind of flammable gas whose major component is methane.[1] If CBM was not utilized and vented into the atmosphere, it not only would bring about air pollution, but also an energy resource would be wasted, because methane in CBM is 21 times more effective than carbon dioxide as a greenhouse gas.[2] At a typical gassy mine, CBM is emitted in three streams: (1) gas drained from the seam before mining (60–95% methane), (2) gas drained from the worked areas of the mine, *e.g.* goafs[3] (30–90% methane), usually mixed some amount of oxygen, and (3) methane ventilation air (0.1–1% methane).[2,4] High concentration drained gas is easy to use; medium concentration CBM (30–80% methane), which mixed with some amount of oxygen, needs to be converted into methane-rich gas, containing at least 96 vol.% methane, and then it can be delivered to local natural gas supply systems. The pressure swing adsorption (PSA) method can be used in practice to recover methane from coal bed gas,[5] in which both methane and oxygen in emissions are concentrated. However it is inevitable that the emissions still contain 5–15% of oxygen, within the limit of methane explosion. So it is necessary to remove oxygen of the medium concentration drained gas before using it. There are two main methods used in the CBM deoxygenation: non-catalytic and catalytic deoxygenation. There are several disadvantages of non-catalytic deoxygenation, such as not removing oxygen thoroughly, operation at high temperature, and producing some by-products. While there are several advantages of catalytic deoxygenation, such as, removing oxygen thoroughly, and operating at low temperature, the choice of catalyst is critical and some methane will be consumed. Comparing the characteristics of the two methods, we choose the latter method to catalytically remove oxygen from CBM. Catalytic deoxygenation is a method which uses methane catalytic combustion to remove oxygen.

Although methane catalytic combustion is a simple reaction, it is a strong exothermic reaction, which would induce temperature runaway of the catalyst bed, resulting in catalyst deactivation due to a catalyst sintering at high temperature. As an option to overcome the catalyst deactivation, lanthanum-transition metal perovskites ($LaMO_3$) have attracted a lot of attention, because of their outstanding hydrothermal stability and high temperature stability.[6]

As a novel catalytic material, perovskite composite oxides (general formula ABO_3) are being extensively researched, especially for the development of combustion catalysts and environmental purification catalysts.[7] Lanthanum cobaltite perovskite as an important one of the perovskite structures oxides attracts wide interest because of its excellent catalytic activity for the oxidation reactions,[8–12] such as for the total

[a] *Key Laboratory for Advanced Materials and Research Institute of Industrial catalysis, East China University of Science and Technology, Shanghai 200237, P. R. China. E-mail: gzhlu@ecust.edu.cn; Fax: +86-21-64253824*
[b] *Research Institute of Applied Catalysis, Shanghai Institute of Technology, Shanghai 200235, P. R. China*

oxidation of methane.[11,12] Rare earth elements have some special chemical properties and are often used as a promoter in a variety of catalysts, to improve the performance of a catalyst. Doping Ce or Nd as an additive in $LaCoO_3$ perovskite can vary its physicochemical properties and improve the catalytic activity.[9,13] Although the catalytic oxidation of methane has been studied extensively, in almost all studies the methane concentration is very low, such as $<0.1\%$, and the oxygen concentration is very high ($>15\%$), in fact, this is a de-methane process. Being different with the catalytic de-methane process above, this paper is focused on the deoxidization of coal bed methane, in which methane concentration is very high and oxygen concentration is low. Therefore, according to the basic requirements for a deoxidization of coal bed methane, we have developed the Er-doped $LaCoO_3$ perovskite catalyst. The research results reveal that the presence of Er can remarkably improve the activity of the $LaCoO_3$ catalyst for the deoxidization of CBM. To the best of our knowledge, there is little research work for the catalytic deoxidization of CBM, especially for the catalytic deoxidization of CBM over the Er-doped $LaCoO_3$ perovskite catalyst, which has not been reported.

Herein, we synthesized a series of perovskite-type $La_{1-x}Er_xCoO_3$ (x = 0.0–0.4) catalysts by a co-precipitation method and the catalysts were characterized by X-ray diffraction (XRD), laser Raman spectroscopy (LRS), H_2 and CH_4 temperature-programmed reduction (H_2, CH_4-TPR), CO pulse and N_2 adsorption/desorption techniques and so on. And taking $La_{0.8}Er_{0.2}CoO_3$ as a model catalyst, the influences of the operational parameters, such as methane concentration, oxygen concentration and space velocity, on the catalytic deoxygenation of CBM and its kinetics behaviours were investigated.

2. Experimental

2.1. Catalyst preparation

The $La_{1-x}Er_xCoO_3$ (x = 0.0, 0.1, 0.2, 0.3 and 0.4) catalysts were prepared by the co-precipitation method. $La(NO_3)_3{\cdot}6H_2O$ and $Co(NO_3)_2{\cdot}6H_2O$ salts were dissolved in de-ionized water (0.3 mol L^{-1} La^{3+} and 0.3 mol L^{-1} Co^{2+}). Then ammonium carbonate (1 mol L^{-1}) aqueous solution was dropped in the above solution under stirring at 60 °C until pH ~9, and the precipitate was obtained and aged in this matrix solution for 4 h at 60 °C under vigorous stirring. After filtering and washing with de-ionized water, the solid product was dried at 120 °C for 12 h and then calcined at 800 °C for 4 h in air.

2.2. Catalyst characterization

Powder X-ray diffraction patterns were performed on a Rigaku D/max 2250VB/PC diffractometer with Cu Kα radiation (λ = 1.540656 Å, scanning step 0.02°) at scanning rate 6° min^{-1}. The BET specific surface areas of catalysts were measured on a NOVA 4200e Surface Area and pore size analyser by N_2 adsorption at −196 °C and Brunauer–Emmett–Teller method. The Raman spectra at 100–1000 cm^{-1} were obtained on a Renishaw Raman spectrometer equipped with a CCD detector at ambient temperature and moisture-free conditions, and the emission line at 514.5 nm from an Ar^+ ion laser was used for excitation and the output laser power was 10 mW.

H_2-temperature-programmed reduction (H_2-TPR) of the sample was carried out in a conventional flow system equipped with a thermal conductivity detector (TCD). 50 mg sample was loaded in the U-shaped quartz tube reactor. 5% H_2/N_2 mixture gas at a flow rate of 45 mL min^{-1} was used and the heating rate was 10 °C min^{-1}.

CH_4-TPR and the CO pulse experiments were conducted in the U-shape quartz tube reactor and the effluent gas was monitored by on-line quadrupole mass spectrometer (MS, IPC 400, INFICON Co. Ltd.). The catalyst was pretreated at 650 °C for 0.5 h in 20% O_2/He of 50 mL min^{-1}, followed by cooling down to room temperature at the same atmosphere. In the testing of CH_4-TPR, 0.5% CH_4/He of 50 mL min^{-1} was used as the reactant gas, and the heating rate was 10 °C min^{-1}. In the CO pulse experiment, the reaction temperature was 410 °C, and the carrier gas was He with a flow rate of 50 mL min^{-1}. After the system reaches equilibrium, 35.62% CO/Ar was pulsed into the reactor system at intervals of 1 min with a loop volume of 1 mL.

2.3. Testing of catalytic activity

The catalytic activities of $La_{1-x}Er_xCoO_3$ catalysts for the catalytic deoxidization of CBM were tested in a stainless steel tube fixed-bed reactor (500 mm × Φ 21mm/inner diameter) at atmospheric pressure. The feed gas was consisted of 30% CH_4 + 6% O_2 + Ar (balance) with 50 mL min^{-1}, and 0.5 g catalyst diluted with 15 g silica sands (20–40 mesh) was used. The weight hourly space velocity (WHSV) was 6000 mL h^{-1} g^{-1}). The reactants and products were analyzed online by a gas chromatograph (GC) equipped with TCD. The catalyst activity was expressed by T_{10}, T_{50} and T_{90} representing the reaction temperatures for the oxygen conversion of 10%, 50% and 90%, respectively.

3. Results and discussion

3.1. Catalyst characterization

The XRD patterns of $La_{1-x}Er_xCoO_3$ (x = 0–0.4) samples with different Er contents are shown in Fig. 1, and their BET

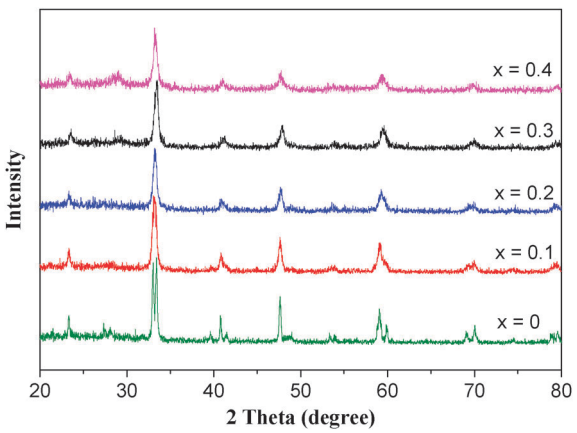

Fig. 1 XRD patterns of $La_{1-x}Er_xCoO_3$ catalysts.

Table 1 BET surface areas (SA), crystallite sizes (d_{110}) of $La_{1-x}Er_xCoO_3$ catalysts and their T_{10}, T_{50} and T_{90}

$La_{1-x}Er_xCoO_3$	T_{10} (°C)	T_{50} (°C)	T_{90} (°C)	d_{110} (nm)	SA ($m^2\ g^{-1}$)
$x = 0$	388	463	500	21.7	9.5
$x = 0.1$	454	418	440	18.7	13.4
$x = 0.2$	324	389	419	18.5	11.9
$x = 0.3$	337	412	446	18.8	14.1
$x = 0.4$	350	415	465	19.7	15.2

surface areas and crystallite sizes are listed in Table 1. In the XRD pattern of $LaCoO_3$, there are the typical diffraction peaks of rhombohedral $LaCoO_3$ perovskite (JCPDS card: 48–0123), and a very weak diffraction peak of La_2O_3 at $2\theta = 27$–$28°$ (JCPDS card: 54-0213). Replacing La^{3+} (ionic radius 1.06 Å) with Er^{3+} (0.88 Å) of a lower cation radius $LaCoO_3$ would decrease the tolerance factor,[14] resulting in the aberration of the perovskite structure and a combine of doublet peaks at around 33°, 41°, 59°, 70°, and 79°. Hence, the diffractograms of the substituted Er for La samples ($La_{1-x}Er_xCoO_3$) are similar to that of Ce, Cu, or Ni partial-substitution onto $LaCoO_3$ perovskite.[14,15] The intensities of the diffraction peaks decrease gradually with an increase in Er amount, which indicates that Er ions enters into the perovskite crystalline lattice and distort the crystalline structure. However, for the $La_{1-x}Er_xCoO_3$ ($x = 0.3$ and 0.4) samples a weak signal of Er_2O_3 at $2\theta \approx 29°$ (JCPDS card: 02–0930) can also be observed, that is to say, with an increase in Er amount some Er ions cannot enter into the lattices. The results in Table 1 show that, the presence of erbium in $La_{1-x}Er_xCoO_3$ increases its BET surface area and decreases the crystallite sizes. The results above indicate that there may bring lattice distortion and crystalline structure change of perovskite when part La^{3+} ions in $LaCoO_3$ are substituted by smaller Er^{3+} ion.

Comparing with X-ray diffraction technique, Raman spectroscopy is very sensitive to structure distortion and oxygen motion, and can be used to investigate an electron excitation for the perovskite-type structure materials. The Raman spectra of $LaCoO_3$ and $La_{0.8}Er_{0.2}CoO_3$ at room temperature are shown in Fig. 2, and there are two similar bands at ~140 and 391 cm^{-1} with different intensities, which are similar to that reported by Popa.[16] The bands intensities of $La_{0.8}Er_{0.2}CoO_3$ are much larger than that of $LaCoO_3$, due to disorder induced by erbium substitution for La and a distortion of the lattice structure. According to the data reported,[16,17] we can assign the band at ~391 and ~140 cm^{-1} to E_g mode symmetry. Compared with the Raman spectrum of $LaCoO_3$, there is a new band at ~328 cm^{-1} in the Raman spectrum of $La_{0.8}Er_{0.2}CoO_3$, which was not found in the Raman spectrum of $LaCoO_3$ and further indicates that erbium substitution leads to structure distortion or oxygen motion of perovskite.

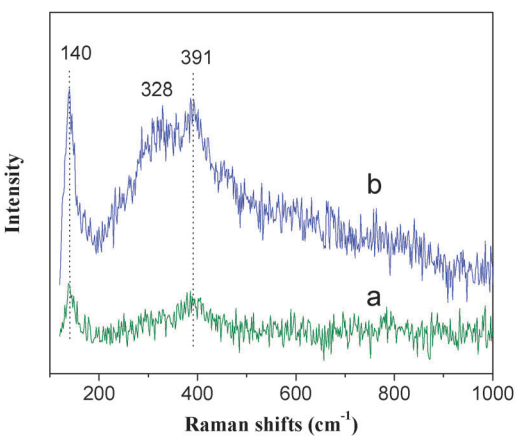

Fig. 2 Raman spectra of $LaCoO_3$ (a) and $La_{0.8}Er_{0.2}CoO_3$ (b).

3.2. H_2-TPR

The H_2-TPR profiles of $La_{1-x}Er_xCoO_3$ catalysts are shown in Fig. 3, and there are two H_2 consumption peaks at 100–800 °C, which correspond to two successive reduction steps. For the perovskite composite oxide, the first step is ascribed to the reduction of M^{3+} to M^{2+} at 100–500 °C,[18,19] and the second step is attributed to the reduction of M^{2+} to metallic state M^0 at 500–800 °C, resulting in a destruction of perovskite structures.[20] Herein, the first step may be corresponding to the reduction of Co^{3+} to Co^{2+} at 300–460 °C and the second reduction step is to the reduction of Co^{2+} to Co^0 at 550–750 °C with a destruction of the perovskite structure.[21–23]

After Er is add in $La_{1-x}Er_xCoO_3$ ($x = 0.1$–0.4), the reduction temperature of the first step declines obviously, and when $x = 0.2$ the reduction peak temperature for the $La_{0.8}Er_{0.2}CoO_3$ sample was down by ~50 °C compared with pure $LaCoO_3$; for the high temperature reduction peak at 600–700 °C, $La_{0.8}Er_{0.2}CoO_3$ is lowest (630 °C) among all samples. The results above show that Er-doped catalysts are reduced more easily by H_2 than pure $LaCoO_3$, that is to say, the lattice oxygen of Er-doped catalysts are more active than pure $LaCoO_3$, and an appropriate doping amount of Er is $x = \sim 0.2$.

3.3. CH_4-TPR

The CH_4-TPR profiles of $La_{1-x}Er_xCoO_3$ catalysts are shown in Fig. 4, and CO_2 ($m/z = 44$) signal was detected by MS. During the CH_4-TPR on $La_{1-x}Er_xCoO_3$ catalysts, the most reactive oxygen species can be removed at low temperatures, and the less reactive oxygen species are only removed at higher temperatures, in which the deep oxidation product CO_2 can be obtained at both stage temperatures.[24]

For the first reaction peak at 150–350 °C, the peak temperature (T_p) of CO_2 desorption over $LaCoO_3$ catalyst is 246 °C, and the presence of Er in $LaCoO_3$ obviously lowers

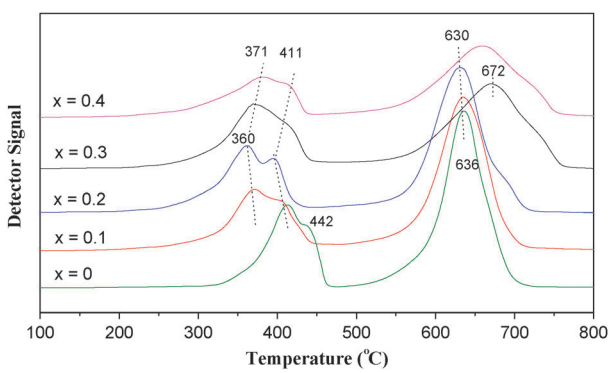

Fig. 3 H_2-TPR profiles of $La_{1-x}Er_xCoO_3$ catalysts.

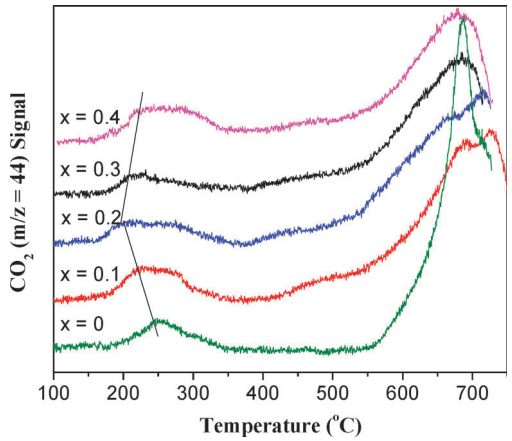

Fig. 4 CO_2 curves in CH_4-TPR on $La_{1-x}Er_xCoO_3$ catalysts.

this peak temperature, for instance, T_p on $La_{0.8}Er_{0.2}CoO_3$ is lowest (194 °C) and T_p on $La_{0.6}Er_{0.4}CoO_3$ is 222 °C, which should be attributed to the reaction of methane with surface oxygen on the catalyst. At 370–530 °C, there is no CO_2 peak on $LaCoO_3$, while there are smaller CO_2 peaks on the Er-doped samples. At >530 °C, the CO_2 peak over Er-doped samples is wider than that on $LaCoO_3$, which is attributed to the reaction of methane with bulk lattice oxygen of the catalyst. The results above indicate that $La_{0.8}Er_{0.2}CoO_3$ has more active surface oxygen and higher amounts of reactive lattice oxygen than $LaCoO_3$. This situation is similar to the results of H_2-TPR.

3.4. CO pulse experiment

The oxygen migrations in $LaCoO_3$ and $La_{0.8}Er_{0.2}CoO_3$ catalysts were investigated by the CO pulse experiment, and the results (CO signal, m/z = 28) are shown in Fig. 5. It can be seen that the unreacted CO (m/z = 28) amount detected on $LaCoO_3$ is much more than that on $La_{0.8}Er_{0.2}CoO_3$, that is, more CO have been converted to CO_2 on $La_{0.8}Er_{0.2}CoO_3$. As the surface oxygen amount is less, pulsed CO is mainly converted by lattice oxygen from the sub-surface and bulk oxygen of the catalyst after the first pulse. The slope of the change in CO signals on $LaCoO_3$ is milder than that on $La_{0.8}Er_{0.2}CoO_3$. These different slopes may be induced by different amounts of the active lattice oxygen, and different reactivities and migration rates of lattice oxygen. The results in Fig. 5 show that the presence of Er in $La_{0.8}Er_{0.2}CoO_3$ increases the amount of the active lattice oxygen and improves obviously the reactivity and migration rate of lattice oxygen in $LaCoO_3$, which is consistent with the results in H_2-TPR and CH_4-TPR.

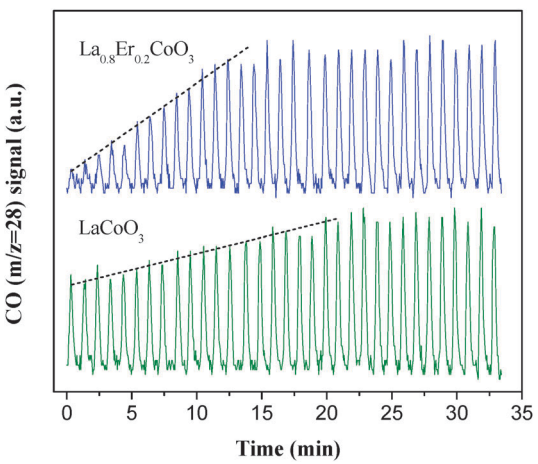

Fig. 5 CO pulse experiment at 410 °C on $LaCoO_3$ and $La_{0.8}Er_{0.2}CoO_3$.

3.5. Catalytic performances of $La_{1-x}Er_xCoO_3$ catalysts for deoxidization of CBM

The effect of Er content (x) on the catalytic performance of $La_{1-x}Er_xCoO_3$ for CBM deoxidization is shown in Fig. 6, in which CO_2 and H_2O are the only products. The results show that the activities of Er-doped catalysts are apparently superior to that of the $LaCoO_3$ catalyst, and when x = 0.2 the $La_{0.8}Er_{0.2}CoO_3$ catalyst presents the maximum activity, for instance, T_{90} (the reaction temperature for 90% O_2 conversion) over $La_{0.8}Er_{0.2}CoO_3$ is ~420 °C, and T_{90} over $LaCoO_3$ is ~500 °C.

The effects of CH_4 and O_2 concentrations on the conversion of O_2 over $La_{0.8}Er_{0.2}CoO_3$ are shown in Fig. 7 and 8. As shown in Fig. 7, increasing methane concentration can increase the O_2 conversion at the same space velocity; contrarily, increasing oxygen concentration decreases the O_2 conversion under the same reaction conditions (Fig. 8).

Methane combustion over the metal oxides catalysts or Pd supported on oxide catalysts is known to follow a redox mechanism, and a variety of kinetic models for the catalytic

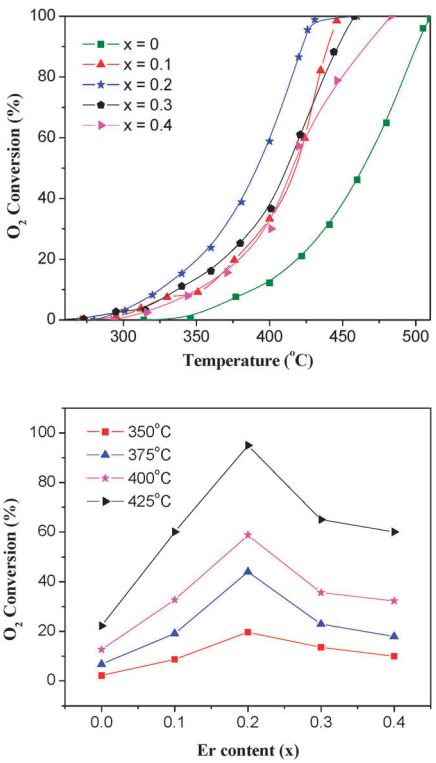

Fig. 6 Effect of Er content on the catalytic activity of $La_{1-x}Er_xCoO_3$ for the deoxidization of CBM. (30% CH_4–6% O_2/Ar balance, WHSV = 6000 mL h^{-1} g^{-1}).

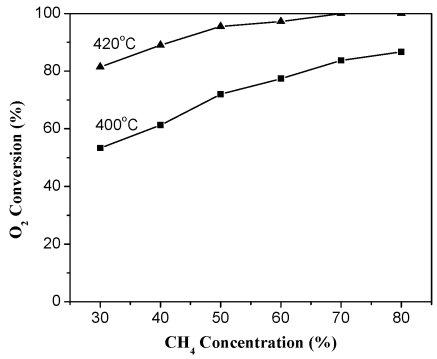

Fig. 7 Effect of CH_4 concentration on the O_2 conversion over $La_{0.8}Er_{0.2}CoO_3$. (6% O_2/Ar balance, WHSV = 6000 mL h^{-1} g^{-1}).

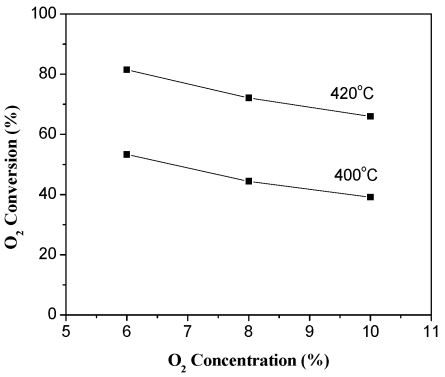

Fig. 8 Effect of O_2 concentration on the O_2 conversion over $La_{0.8}Er_{0.2}CoO_3$. (30% CH_4/Ar balance, WHSV = 6000 mL h^{-1} g^{-1}).

combustion of methane were reported,[25–30] which is related to the reaction mechanisms of Rideal–Eley, or Langmuir–Hinshelwood bi-molecules, or Mars–van Krevelen, or purely empirical expression. In general, in studying the kinetic models for the catalytic combustion of methane, a low concentration methane and excess oxygen were adopted, which is as a model of VOCs (volatile organic compounds) purification, that is to say, it is a process of de-methane. Herein we focus on a deoxygenation of CBM, so that in the condition of high concentration and excess methane the kinetic behaviours for the catalytic combustion of methane over the $La_{0.8}Er_{0.2}CoO_3$ catalyst were investigated. Although the general equation for methane combustion is relatively complex, by the help of the empirical kinetic expression the rate equation of removing oxygen by the catalytic combustion of methane can be obtained as follows:

$$r = \mathrm{k}P^{a}_{\mathrm{CH_4}}P^{b}_{\mathrm{O_2}}P^{c}_{\mathrm{H_2O}}P^{d}_{\mathrm{CO_2}} \quad (1)$$

Based on the facts that CO_2 and H_2O are the products in the methane combustion, their concentrations in the feed gases were almost zero and the oxygen conversion at 320 °C is $<13\%$, $P^{c}_{\mathrm{H_2O}}$ and $P^{d}_{\mathrm{CO_2}}$ can be supposed to be approximately constant, while eqn (1) can be simplified as:

$$r = \mathrm{k}P^{a}_{\mathrm{CH_4}}P^{b}_{\mathrm{O_2}} \quad (2)$$

Taking the logarithm of eqn (2), eqn (3) can be obtained:

$$\ln r = a \ln P_{\mathrm{CH_4}} + b \ln P_{\mathrm{O_2}} + \ln \mathrm{k} \quad (3)$$

In the conditions of 30–80% CH_4 and 6% O_2 at a space velocity (WHSV) of 6000 mL h^{-1} g^{-1}) and 320 °C, eqn (3) can be simplified to $\ln r = a \ln P_{\mathrm{CH_4}} + C$; $\ln r$ against $\ln P_{\mathrm{CH_4}}$ over the $La_{0.8}Er_{0.2}CoO_3$ catalyst at 320 °C has been plotted in Fig. 9. The slope of the straight line, a is $\sim$0.9. In the conditions of 6–10% O_2 and 30% CH_4 at a space velocity (WHSV) of 6000 mL h^{-1} g^{-1}) and 320 °C, eqn (3) can be simplified to $\ln r = b \ln P_{\mathrm{O_2}} + C$; $\ln r$ against $\ln P_{\mathrm{O_2}}$ over the $La_{0.8}Er_{0.2}CoO_3$ catalyst at 320 °C has been plotted in Fig. 10. The slope of the straight line, b is ~ -0.6. It is found that the order of removing O_2 for methane concentration is 0.9, in agreement with the first order found in literatures;[30–33] and the order for oxygen concentration is −0.6, unlike zero order for oxygen reported in the literature.[30,33] This can be explained that methane is adsorbed on oxygen vacancies on the surface. These vacancies can be occupied by molecular oxygen in a linear way of $O_2(g) + * \rightarrow O_2*$, and then by atomic oxygen of $O_2* + * \rightarrow 2O*$, resulting in the number of vacancies being dependent on the pressure $P_{\mathrm{O_2}}$ of the gas phase, that is, the reaction rate of removing O_2 is dependent on $P_{\mathrm{O_2}}$. As $P_{\mathrm{O_2}}$ pressure increases, the number of vacancies decreases and the order with respect to $P_{\mathrm{O_2}}$ is negative. This is the pseudo-Langmuir–Hinshelwood mechanism proposed by Iglesia *et al.*[34,35] It is interesting that based on the pseudo-Langmuir–Hinshelwood mechanism, the results calculated by a Monte Carlo simulation for the catalytic oxidation of methane shows that the order for oxygen is −0.62,[30] being the same as the order of oxygen here. It is understandable that, for the bi-molecules reaction followed Langmuir–Hinshelwood mechanism, the reaction would be subjected to limitation if one of the reactants adsorbed very strongly on the active sites competitively against another reactant, and hence we can deduce that an adsorption of methane should be the rate-determining step, which should be attributed to the catalytic combustion kinetics behaviours for high concentration methane (deoxygenation) being different from that for very low concentration methane (de-methane).

The effect of space velocity on the O_2 conversion over $La_{0.8}Er_{0.2}CoO_3$ catalyst is shown in Fig. 11. It indicates that, at the same reaction conditions a lower space velocity results in higher O_2 conversion. This is because lower space velocity gives longer residence times of reactant gases in the catalyst bed.

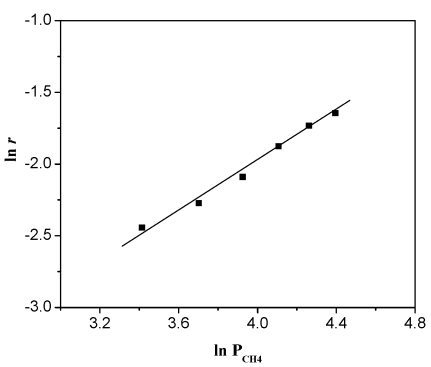

Fig. 9 $\ln r$ as a function of $\ln P_{\mathrm{CH_4}}$ over $La_{0.8}Er_{0.2}CoO_3$ at 320 °C. (The feed gas consisted of 30–80% CH_4 and 6% O_2 at a space velocity (WHSV) of 6000 mL g^{-1} h^{-1}), the conversion of O_2 was adjusted to below 13%).

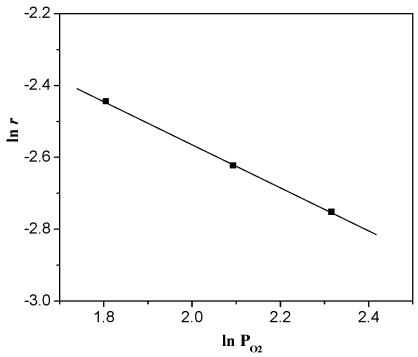

Fig. 10 ln r as a function of ln P_{O_2} over $La_{0.8}Er_{0.2}CoO_3$ at 320 °C. (The feed gas consisted of 6–10% O_2 and 30% CH_4 at a space velocity (WHSV) of 6000 mL h^{-1} g^{-1}), the conversion of O_2 was adjusted to below 6%).

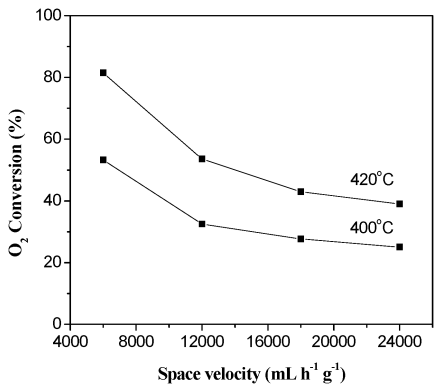

Fig. 11 Effect of space velocity on the O_2 conversion over $La_{0.8}Er_{0.2}CoO_3$. (30% CH_4–6% O_2/Ar balance).

4. Conclusions

For medium concentration drained gas (30–80% CH_4) mixed with some oxygen, oxygen should be removed before using it to avoid an explosion. For the catalytic deoxygenation of CBM over perovskite catalysts, the effective $La_{1-x}Er_xCoO_3$ (x = 0–0.4) perovskite catalysts were prepared successfully. The results show that the partial substitution of La by Er modifies the rhombohedral structure of the $LaCoO_3$ perovskite and promotes its activity of lattice oxygen, thereby, improving its reactivity for deoxidization of CBM. When x = 0.2, the $La_{0.8}Er_{0.2}CoO_3$ perovskite catalyst possesses higher amounts of active lattice oxygen and higher migration capability of lattice oxygen, resulting in the highest activity for CBM deoxidization among all $La_{1-x}Er_xCoO_3$ catalysts.

The influences of operation parameters, such as methane concentration, oxygen concentration and space velocity, on the activity of $La_{0.8}Er_{0.2}CoO_3$ catalyst for CBM deoxygenation were investigated. The results show that increasing methane concentration can increase the oxygen conversion, and increasing oxygen concentration conversely decreases the oxygen conversion. The study on the kinetics for CBM deoxygenation over $La_{0.8}Er_{0.2}CoO_3$ catalyst indicates that the reaction order of removing oxygen is 0.9 for methane partial pressure and −0.6 for oxygen partial pressure.

Acknowledgements

This project was supported financially by the National Basic Research Program of China (2010CB732300), and the "Shu Guang" Project (10GG23) and Leading Academic Discipline Project (J51503) of Shanghai Municipal Education Commission and Shanghai Education Development Foundation.

Notes and references

1 G. J. Li, *Procedia Earth and Planetary Science*, 2009, **1**, 94.
2 B. Stasińska and A. Machocki, *Pol. J. Chem. Technol*., 2007, **9**, 29.
3 Goaf (pl. Goafs or Goaves): That part of a mine from which the mineral has been partially or wholly removed; the waste left in old workings;—called also {gob}. [1913 Webster] http://www.theenglishdictionary.org/definition/goafs.
4 S. Su and J. Agnew, *Fuel*, 2006, **85**, 1201.
5 A. Olajossy, A. Gawdzlk, Z. Budner and J. Dula, *Chem. Eng. Res. Des*., 2003, **81**, 474.
6 G. S. Gallego, J. G. Marín, C. B. Dupeyrat, J. Barrault and F. Mondragón, *Appl. Catal., A*, 2009, **369**, 97.
7 D. S. Qiao, G. Z. Lu, X. H. Liu, Y. Guo, Y. Q. Wang and Y. L. Guo, *J. Mater. Sci*., 2011, **46**, 3500; L. L. Zhu, G. Z. Lu, Y. Q. Wang, Y. Guo and Y. L. Guo, *Chin. J. Catal*., 2010, **31**, 1006.
8 N. A. Merino, B. P. Barbero, P. Grange and L. E. Cadús, *J. Catal*., 2005, **231**, 232.
9 S. Khan, R. J. Oldman, S. A. French and S. A. Axon, *J. Phys. Chem. C*, 2008, **112**, 12310.
10 J. Li, L. Zhao and G. Z. Lu, *Ind. Eng. Chem. Res*., 2009, **48**, 641.
11 L. Fabbrini, I. Rossetti and L. Forni, *Appl. Catal., B*, 2006, **63**, 131.
12 C. Q. Chen, W. Li, C. Y. Cao and W. G. Song, *J. Mater. Chem*., 2010, **20**, 6968; I. Rossetti, C. Bif and L. Forni, *Chem. Eng. J*., 2010, **162**, 768.
13 M. S. Cui, M. L. Li, S. L. Zhang, Z. Q. Long, D. L. Cui and X. W. Huang, *J. Rare Earths*, 2004, **22**, 623; H. Taguchi, S. Matsuoka, M. Kato and K. Hirota, *J. Mater. Sci*., 2009, **44**, 5732.
14 M. Ghasdi, H. Alamdari, S. Royer and A. Adnot, *Sens. Actuators, B*, 2011, DOI: 10.1016/j.snb.2011.04.003.
15 B. Białobok, J. Trawczynski, W. Mista and M. Zawadzki, *Appl. Catal., B*, 2007, **72**, 395; N. Tien-Thaoa, H. Alamdarib and S. Kaliaguine, *J. Solid State Chem*., 2008, **181**, 2006; X. D. Yang, S. Li, Y. Liu, X. Z. Wei and Y. N. Liu, *J. Power Sources*, 2011, **196**, 4992.
16 M. Popa, J. Frantti and M. Kakihana, *Solid State Ionics*, 2002, **154–155**, 135; M. Popa and J. M. C. Moreno, *Thin Solid Films*, 2009, **517**, 1530.
17 E. Granado, N. O. Moreno, A. Garcia, J. A. Sanjurjo, C. Rettori, I. Torriani, S. B. Oseroff, J. J. Neumeier, K. J. McClellan, S. W. Cheong and Y. Tokura, *Phys. Rev. B: Condens. Matter*, 1998, **58**, 11435.
18 B. Levasseur and S. Kaliaguine, *Appl. Catal., B*, 2009, **88**, 305; S. Royer, F. Berube and S. Kaliaguine, *Appl. Catal., A*, 2005, **282**, 273.
19 J. L. G. Fierro, M. A. Pena and L. G. Tejuca, *J. Mater. Sci*., 1988, **23**, 1018; A. Baiker, P. E. Martin, P. Keusch, E. Fritsch and A. Reller, *J. Catal*., 1994, **146**, 268.
20 M. Crespin and W. K. Hall, *J. Catal*., 1981, **69**, 359.
21 Y. G. Wang, J. W. Ren, Y. Q. Wang, F. Y. Zhang, X. H. Liu, Y. Guo and G. Z. Lu, *J. Phys. Chem. C*, 2008, **112**, 15293.
22 N. A. Merino, B. P. Barbero, C. Cellier, J. A. Gamboa and L. E. Cadus, *Catal. Lett*., 2007, **113**, 130.
23 S. Royer, H. Alamdari, D. Duprezc and S. Kaliaguine, *Appl. Catal., B*, 2005, **58**, 237.
24 V. A. Sadykov, T. G. Kuznetsova, G. M. Alikina, Y. V. Frolova, A. I. Lukashevich, Y. V. Potapova, V. S. Muzykantov, V. A. Rogov, V. V. Kriventsov, D. I. Kochubei, E. M. Moroz, D. I. Zyuzin, V. I. Zaikovskii, V. N. Kolomiichuk, E. A. Paukshtis, E. B. Burgina, V. V. Zyryanov, N. F. Uvarov, S. Neophytides and E. Kemnitz, *Catal. Today*, 2004, **93–95**, 45.
25 V. C. Belessi, A. K. Ladavos and P. J. Pomonis, *Appl. Catal., B*, 2001, **31**, 183.

26 V. C. Belessi, A. K. Ladavos, G. S. Armatas and P. J. Pomonis, *Phys. Chem. Chem. Phys*., 2001, **3**, 3856.
27 S. Specchia, F. Conti and V. Specchia, *Ind. Eng. Chem. Res*., 2010, **49**, 11101.
28 N. Bahlawane, *Appl. Catal., B*, 2006, **67**, 168.
29 T. N. Angelidis and V. Tzitzios, *Stud. Surf. Sci. Catal*., 1999, **122**, 341.
30 J. Cortes, E. Valencia and P. Araya, *Catal. Lett*., 2006, **112**, 121.
31 J. G. Deng, L. Zhang, H. X. Dai, H. He and C. T. Au, *Appl. Catal., B*, 2009, **89**, 87.
32 M. V. Bukhtiyarova, A. S. Ivanova, E. M. Slavinskaya, L. M. Plyasova, V. A. Rogov, V. V. Kaichev and A. S. Noskov, *Fuel*, 2011, **90**, 1245.
33 W. Sheng, D. N. Gao, C. X. Zhang, Z. S. Yuan, P. Zhang and S. D. Wang, *Prog. Chem*., 2008, **26**, 789.
34 K. Fujimoto, F. H. Ribeiro, M. Avalos-Borja and E. Iglesia, *J. Catal*., 1998, **179**, 431.
35 J. Au-Yeung, K. Chen, A. T. Bell and E. Iglesia, *J. Catal*., 1999, **188**, 132.

